EXAFS, Raman and ^{31}P NMR study of amorphous titanium phosphates

C. Schmutz [a], P. Barboux [a,*], F. Ribot [a], F. Taulelle [a], M. Verdaguer [b], C. Fernandez-Lorenzo [c]

[a] *Chimie de la Matière Condensée, URA CNRS 1466, Université P. et M. Curie, 4 Place Jussieu (T54-E5), 75252 Paris cédex, France*
[b] *Chimie des Métaux de Transition, URA CNRS 419, Université P. et M. Curie, 4 Place Jussieu, 75252 Paris cédex, France*
[c] *Departamento de Estructura y Propiedades de Los Materiales, Universidad de Cadiz, Cadiz, Spain*
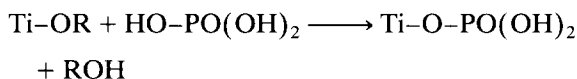
Abstract

The reaction of phosphoric acid with titanium alkoxides for a PO_4/Ti ratio ranging from 0.5 to 2 was investigated. For these compositions, amorphous precipitates are obtained. Their microstructure has been studied by means of Raman, nuclear magnetic resonance and X-ray absorption spectroscopies. The phosphatation of titanium alkoxide increases the Ti coordination number to 6 and the symmetry becomes purely octahedral for a P/Ti ratio of 2. For the composition range $0 < PO_4/Ti \leqslant 2$, phosphate anions are homogeneously dispersed in the precipitate and bound to titanium, the coordination of which is completed by oxo-, hydroxo- and remaining alkoxy- groups. Short Ti–O distances are observed in the materials having the lowest P/Ti ratios.
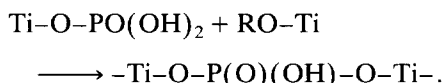
1. Introduction

Titanium phosphates have a wide range of technological applications such as ionic exchangers ($\alpha Ti(HPO_4)_2$–H_2O) [1], ionic conductors [2] and materials having non-linear optical properties such as the crystalline $KTiOPO_4$ phase [3]. Amorphous semiconducting glasses are also found in the same phase diagram [4,5]. We have studied the synthesis of such materials by solution techniques through reaction of anhydrous phosphoric acid with titanium alkoxides. These reactions of phosphatation involve a mechanism such as [6]

$$Ti–OR + HO–PO(OH)_2 \longrightarrow Ti–O–PO(OH)_2 + ROH$$

followed by

$$Ti–O–PO(OH)_2 + RO–Ti$$
$$\longrightarrow -Ti–O–P(O)(OH)–O–Ti–.$$

This reaction corresponds to a nucleophilic substitution of alkoxy group by phosphate and leads to the formation of three-dimensional Ti–O–P–O–Ti–O–P networks by condensation reactions. Such mechanisms offer an alternative to the well known hydrolysis–condensation sequences described in conventional sol–gel processes and in-

---

organic polymerization. Indeed, gels and colloidal solutions of titanium phosphates can be obtained without any hydrolysis [7,8].

Therefore, the formation of solid hetero-condensed networks (composed of both tetrahedral PO_4 and octahedral TiO_6 groups) may be compared with the homo-condensation of pure titanium oxide after hydrolysis. Also, the question arises as to the type of phosphate species involved in the condensation process (PO_4^{3-}, HPO_4^{2-},...) and how the coordination of titanium and the acidity of phosphate groups change upon increasing the P/Ti ratio. We describe in this paper the precipitation of titanium ethoxide by anhydrous phosphoric acid.

2. Experiments and results

2.1. Experimental procedure

Starting solutions were prepared by dissolving solid anhydrous H_3PO_4 (Fluka) and titanium ethoxide (Fluka) in pure ethanol (Prolabo, Normapur) at a concentration of 1 mol dm^{-3}. Measurements on the phosphoric acid solution were made after 1 week and 1 month of aging using liquid state ^{31}P Nuclear magnetic resonance (NMR). Only one signal is observed at +1.8 ppm, referenced to H_3PO_4 85% in water. This signal is attributed to partially ionized H_3PO_4 but no esters of ethanol and phosphoric acid ($PO(OH)_{3-x}(OEt)_x$, $x = 1$, 2 or 3), the characteristic feature of which contains a coupling with the neighbouring protons, are detected [6]. Therefore, the solution contains only pure orthophosphoric acid in ethanol. Note that the fact that no esterification occurs also implies the absence of water. Indeed, Karl Fisher analysis performed on the solution aged for 2 months yields a ratio $H_2O/P = 0.05$.

Addition of the appropriate amount of phosphoric acid to titanium alkoxide was performed under rapid stirring. A white precipitate formed in all cases. Upon aging, sedimentation occurred for nominal compositions P/Ti < 1 and P/Ti > 2, whereas the samples remained homogeneous and gelatinous for the ratios 1 < P/Ti < 2. The samples were centrifuged and the solid part was dried in air at 70°C. Since chemical analysis shows that only residual carbon is left in the precipitates (less than 0.2 ethoxy groups for one Ti for all P/Ti ratios), we conclude that the remaining alkoxy groups have been removed by hydrolysis with the air moisture. In order to elucidate the effect of this drying step, especially from the hydrolysis point of view, the local structure of the wet precipitates was also investigated. In the following, 'gels' refers to the wet samples and 'precipitates' refers to the dried samples.

2.2. Chemical analysis

Chemical analysis was performed at the CNRS chemical analysis facility in Vernaison, France. H, C, Ti and P were titrated. In the following, the P/Ti ratio always refers to the starting ratios of P and Ti that were mixed in the solutions.

For $1/2 \leqslant P/Ti \leqslant 2$, the ratio of $(P/Ti)_{meas}$ measured in the amorphous precipitates is slightly higher than the nominal composition, as shown in Fig. 1. Therefore, a small amount of the titanium precursor has not been trapped in the solid network. Above the ratio P/Ti = 2, free orthophosphoric acid is observed in the solid state NMR spectrum, indicating that the P/Ti = 2 ratio is the highest that can be precipitated with a stoichiometric composition corresponding to the starting composition.

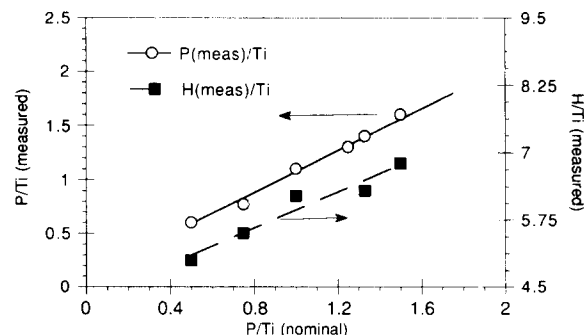Fig. 1. Chemical analysis as a function of nominal P/Ti ratio for P_{meas}/Ti and H_{meas}/Ti.

2.3. X-ray absorption study

2.3.1. Data analysis

X-ray absorption spectra were recorded in the transmission geometry at LURE (Orsay) using the EXAFS III facility equipped with a mono-chromator made of two Si (311) crystals. Samples were prepared in two ways: precipitates were dispersed on a scotch tape and gels were placed in a cell equipped with kapton (12 μm) windows. Three spectra of each sample were taken and averaged together. Data acquisition was at the Ti K edge over the energy range 4950 – 5050 eV by 0.25 eV steps for the absorption edge measurements and over the range 4800–5800 eV by 2 eV steps for the extended X-ray absorption fine structure (EXAFS) acquisitions. The absorption edges were calibrated in energy by recording a Ti metal foil between each sample. The EXAFS spectra were transformed and studied using the computer programs written by Michalowicz [9]. In order to facilitate the comparison between samples, all mathematical treatments of the spectra were chosen to be similar: the background absorption was approximated from the pre-edge region using a straight line and atomic absorption was fitted between 4870 and 5600 eV with a fifth degree polynom. EXAFS signals, $k\chi(k)$, where k is the wave vector, were then extracted using the Lengeler–Eisenberger formula. Fourier transformation of the $k^3\chi(k)$ signals was performed between 2 and 12 $\mathring{A}^{-1}$ using a Kaiser window. Amplitude and phase shifts functions were taken from the calculations performed by McKale et al. [10].

We simulated in this analysis only the peak between 1.0 and 2.0 $\mathring{A}$ of the Fourier transforms. This choice was due to the difficulty in fitting the very weak peaks composed of a mixture of the contribution of different second neighbours (O, P, Ti) at many slightly different distances. Even the fit on crystalline $\alpha Ti(HPO_4)_2$–H_2O failed to give significant results for the second coordination sphere of Ti. Therefore, all samples were examined for the average distance and number of neighbours associated with the first coordination sphere.
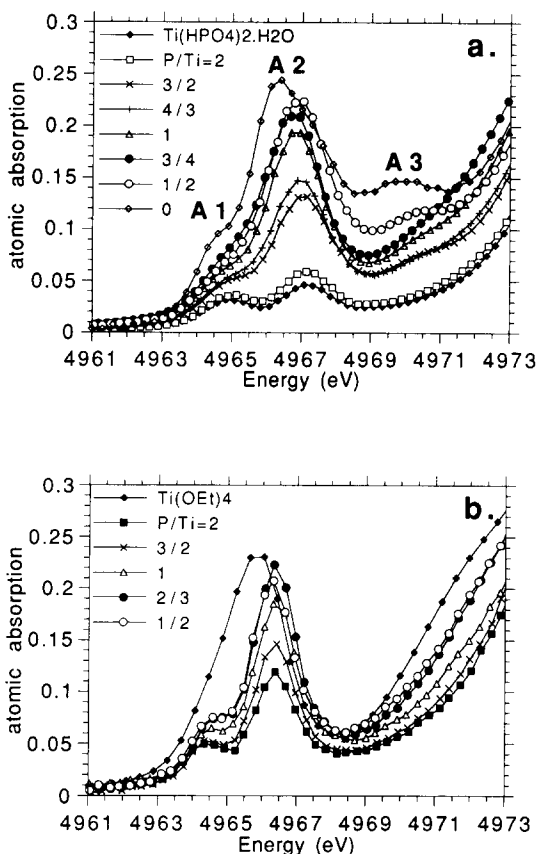

Fig. 2. Near-edge X-ray absorption spectra: (a) precipitates compared with $\alpha Ti(HPO_4)_2$–H_2O; (b) gels. (The first maximum of the absorbance of the metallic titanium edge is taken as a reference at 4964.2 eV.)

2.3.2. Near-edge absorption

Some characteristic absorption spectra as well as the spectra of hydrous TiO_2–nH_2O and crystalline $\alpha Ti(HPO_4)_2$–H_2O are displayed in Fig. 2(a). For comparison, all spectra have been normalized to the absorption at 5030 eV (in a flat part of the spectra, after the edge). In all precipitates studied, the spectrum shows a very weak pre-edge (as compared with the intensity of the absorption edge) consisting of three peaks (A1, A2, A3). The intensity of the peak A2 as a function of the P/Ti ratio is reported in Fig. 3. Upon increasing the P/Ti ratio, the intensity of the A2 and A3 peaks continuously decreases.

The gels, obtained immediately after reaction of phosphoric acid and $Ti(OEt)_4$ without hydroly-
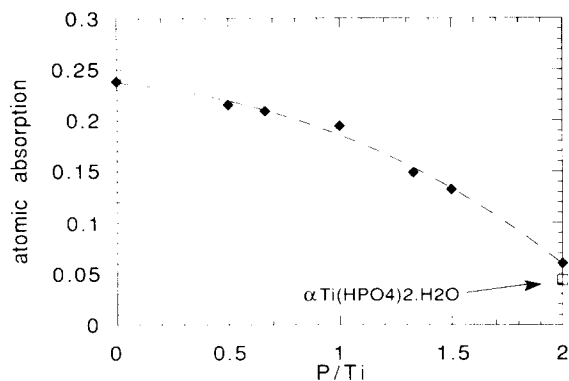
Fig. 3. Variation of the intensity of the A2 peak as a function of the P/Ti ratio in the case of precipitates. (The line is a guide to the eye.)

sis, yield spectra which are similar (Fig. 2(b)). However, the A2 and A3 absorption have a quite high intensity as compared with the corresponding precipitates, especially for the P/Ti = 2 ratio.

2.3.3. EXAFS study of the gels

We first report on the samples obtained before hydrolysis and drying in air (gels). The Fourier transform of the EXAFS spectra yields the pseudo-radial distribution function. These are complex numbers and only the modulus of each is shown in Fig. 4(a), for different P/Ti ratios. On each Fourier transform, intense peaks are observed at short distances. These peaks can be simulated by the scattering of six first oxygen neighbours at short distances (1.80–2.00 Å). The distances were obtained from fits on the EXAFS signals. Calculated curves obtained from these fits are reported in Fig. 4(b).

The numerical results from the fits of the EXAFS spectra are reported in Fig. 5. For the low P/Ti ratios, we observe short Ti–O bond distances (1.85 Å) and larger ones (2.02 Å). Upon increasing the P/Ti ratio, the number of short Ti–O bonds decreases and the coordination of Ti exhibits a higher symmetry as observed in Figs. 5(a) and (b). The average Ti–O distance for P/Ti = 2 is 1.97 Å.

2.3.4. EXAFS study of the precipitates

A similar trend is observed in the precipitates but they exhibit a different aspect. The Fourier

transforms are reported in Fig. 6. In the sample corresponding to the P/Ti = 1/2 ratio, we clearly observe two different Ti–O distances located around 1.94 and 2.06 Å. However, for the higher ratios, only one single peak is observed. The intensity of this peak increases upon increasing the phosphate content. We attribute this behaviour to an increasing ordering around Ti. Indeed, for the low P/Ti ratio, there is a wide distribution of Ti–O sites. This distribution results in a non-constructive sum of EXAFS modulations in the absorption spectra and yields a weak intensity of the EXAFS signals and of the Fourier transforms as well. The effect of disorder
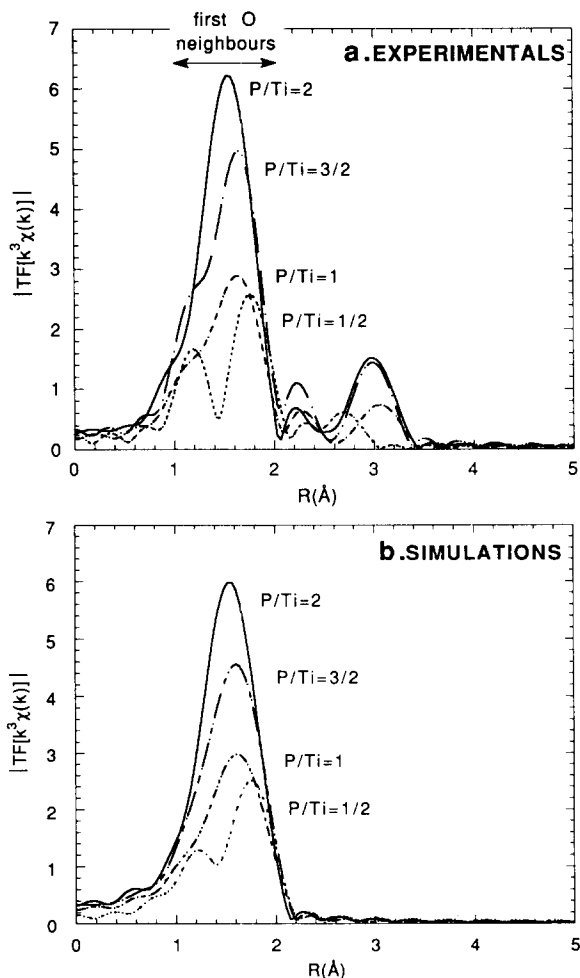

Fig. 4. Fourier transforms of EXAFS spectra for the gels: (a) experimental and (b) simulated.
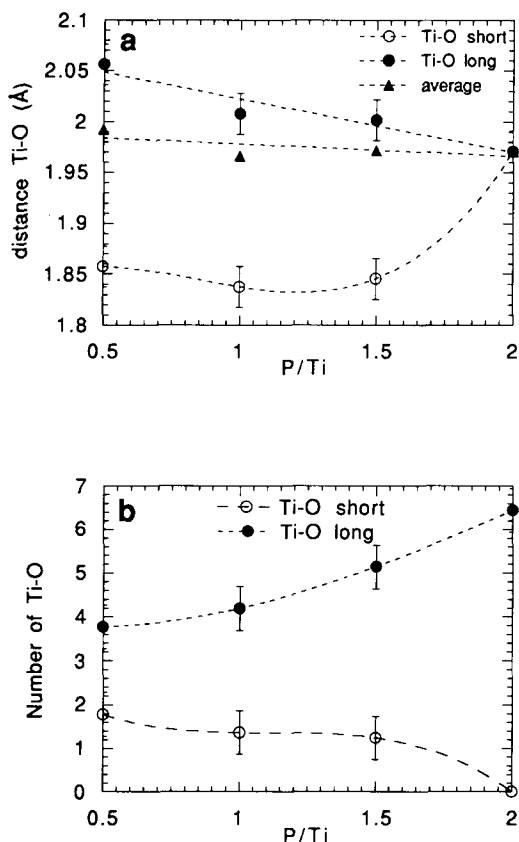
Fig. 5. EXAFS analysis of the gels: (a) distance of oxygen first neighbours and; (b) number of oxygen at these distances as a function of the P/Ti ratio. (Lines are guides to the eye.)
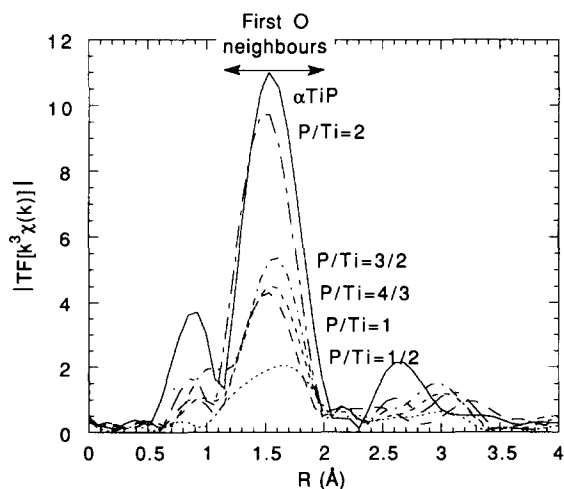

Fig. 6. Fourier transforms of EXAFS spectra for the precipitates.

(thermal and in this case mostly static) on the EXAFS spectra has been largely discussed elsewhere [11,12]. Here, we have a broad distribution of Ti–O distances whereas in the gels they are split in two well defined types (short and long). Therefore, in the case of the precipitates only the average Ti–O distance can be obtained from the fits.

Fig. 7 shows the average Ti–O distance as a function of the P/Ti ratio deduced from the fits to the single Ti–O peak. A monotonic decrease from 2.04 Å to 1.96 Å is observed when going from P/Ti = 0.5 up to 2. For comparison, we also plot the experimental result for crystallized $\alpha Ti(HPO_4)_2 - H_2O$ that has been fitted with a single oxygen peak at 1.95 Å, in good agreement with the average Ti–O distances obtained from the crystallographic determination [13].

The Ti–O distance observed in the precipitate $TiO_2 - nH_2O$, obtained by precipitation of $Ti(OEt)_4$ by water, is large (2.00 Å). This value better corresponds to bridging Ti–OH bonds than to the Ti–O distances observed in the oxide (typically 1.90 Å). Thus, it should be more appropriate to write a formula such as $Ti(O)_{2-x}(OH)_{2x} - (n - x)H_2O$, since the material may still contain a large amount of uncondensed TiOH groups. However, another hypothesis is that the effect of disorder on the decrease of the EXAFS intensity may be stronger for the shorter Ti–O distances. This would explain a higher contribution to the
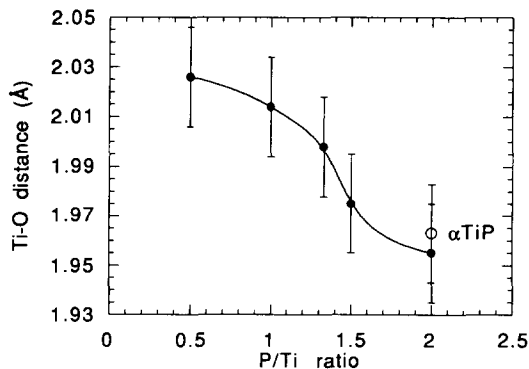

Fig. 7. Distance of oxygen first neighbours for precipitates compared with $\alpha Ti(HPO_4)_2 - H_2O$. (The line is a guide to the eye.)

spectrum of the long Ti–O distances and the apparently high average Ti–O distance observed.

2.3.5. ^{31}P NMR

^{31}P solid state magic angle spinning (MAS)-NMR spectra have been recorded at room temperature on a Bruker MSL 400 spectrometer at the frequency of 161.98 MHz. Samples were spun at a speed of ~ 7 kHz. The chemical shifts are referenced to H_3PO_4 85% in water. NMR spectra are reported in Fig. 8 for different compositions. For the lower P/Ti ratios, broad peaks are observed, obviously composed of several contributions. For the P/Ti = 1 composition, a better resolution allows the decomposition of the broad peaks into peaks located around − 4.4, − 9.3 and − 14.7 ppm. These peaks correspond to different connectivities of the phosphate ion. For the P/Ti = 2 composition, a major peak is observed at − 21.7 ppm. Simulation of all spectra yields the percentage of each signal as a function of the P/Ti ratio. Results are reported in Fig. 9(a).

2.3.6. Raman spectroscopy

The precipitates were investigated using Raman spectroscopy with an argon laser operating at the 514.5 nm wavelength (SpectraPhysics 168) and a detection system Jobin Yvon (U-1000).

Results obtained on the precipitates with different P/Ti ratios are displayed in Fig. 10. In the case of the hydrous precipitate obtained from hydrolysis of titanium tetraethoxide, strong vibrations peaks are observed at 610, 440 and 248 cm^{-1}. This spectrum is similar to those obtained for the crystalline forms of TiO_2 [14]. In particular the position of the Ti–O stretching mode at 610 cm^{-1} is characteristic of an octahedral TiO_6 complex (peaks are located at 610 and 640 cm^{-1} in rutile and anatase, respectively). This position indicates an average Ti–O interatomic distance between 1.94 and 1.97 Å as in the two crystalline forms. In the sample having the P/Ti = 2 ratio, the spectrum is also similar to the signal observed for the crystalline $\alpha Ti(HPO_4)_2$–H_2O structure which is also shown in Fig. 10. Due to the amor-

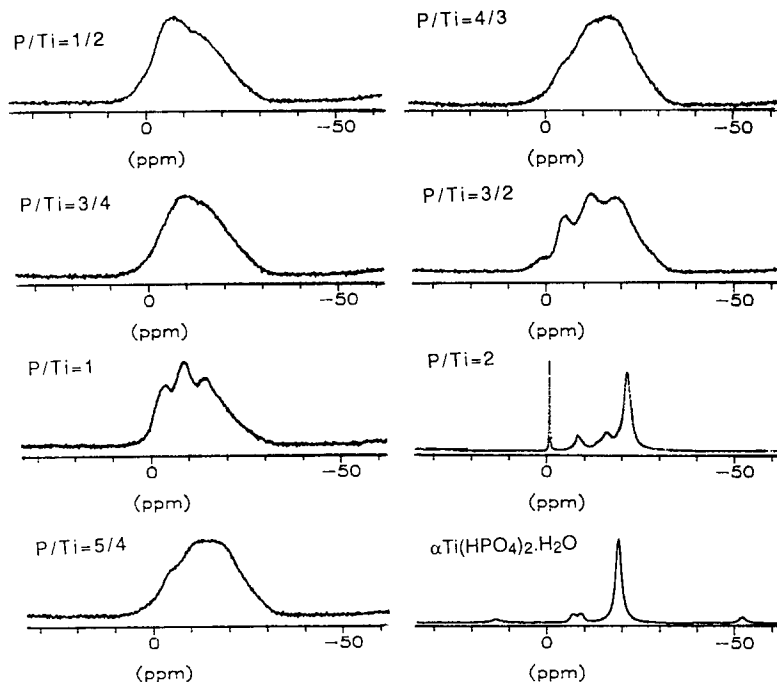Fig. 8. ^{31}P NMR spectra of different compositions P/Ti and $\alpha Ti(HPO_4)_2$–H_2O.

phous state, broad peaks are observed. This structure has been already investigated in the Zr-analog by Horsley et al. [15]. Characteristic vibrations of the PO_4 molecular units are observed around 1000 cm^{-1} (P–O symmetrical and asymmetrical stretchings), 532 cm^{-1} (O–P–O bending) and 319 cm^{-1} (OPO rocking). The remaining vibrations may be attributed to the TiO_6 units. They are observed at 568, 411 and 259

cm^{-1}. The energy of the Ti–O stretching vibration (568 cm^{-1}) is quite low as compared with crystalline TiO_2, probably indicating a rather long bond length. For the intermediate compositions and upon increasing the P/Ti ratios, a decrease of the bands characteristic of the hydrous titanium oxide is observed, whereas the peaks characteristic of the phosphate units grow.
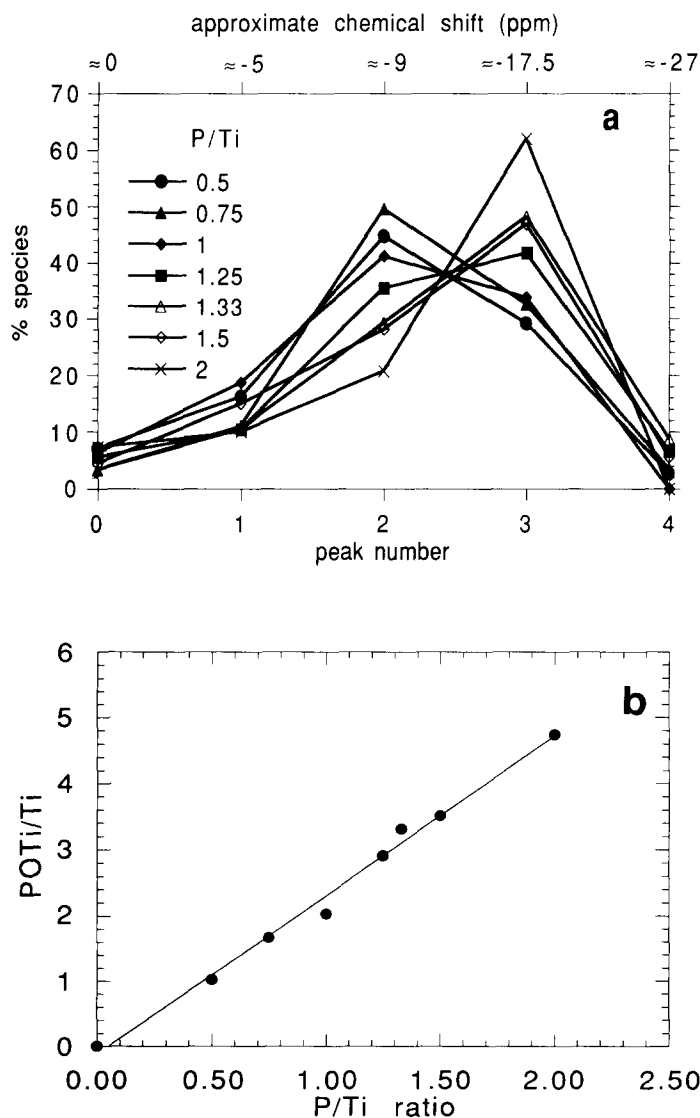
However, for the P/Ti ratios < 2, the most

Fig. 9. (a) Analysis of ^{31}P NMR spectra populations. (b) Number of phosphate groups coordinated to each titanium as a function of the P/Ti ratio.
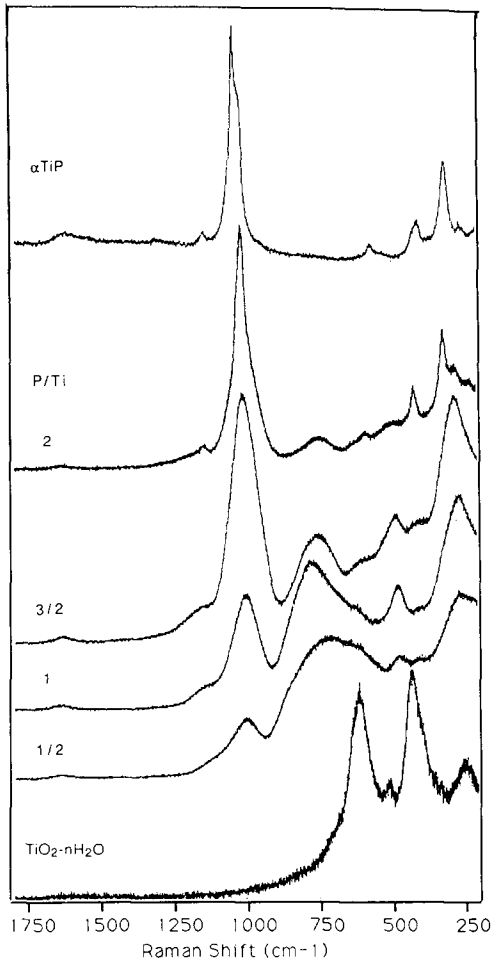
Fig. 10. Raman spectra of different compositions P/Ti and αTi(HPO$_4$)$_2$–H$_2$O.

striking feature of these Raman spectra is the intense vibration observed at 750 cm^{-1}. The highest intensity is observed for the low P/Ti contents. It is not observed for the P/Ti = 0 and 2 compositions.

3. Discussions

3.1. Chemical composition of the precipitates

The chemical composition (P/Ti) shown in Fig. 1 is not far from the theoretical one and we may still consider that all Ti and P have been

trapped in a solid network. The (H/Ti)$_{meas}$ ratios given in Fig. 1 do not take into account the residual organics (correction was made assuming that all the detected carbon is in remaining C$_2$H$_5$O groups). Therefore, these values correspond only to H$_x$PO$_4^{-(3-x)}$, OH$^-$ or H$_2$O groups.

The electroneutrality rule implies the relationship

$$5(P/Ti)_{meas} + (H/Ti)_{meas} + 4 = 2(O/Ti)_{calc}. \tag{1}$$

The plot of (H/Ti)$_{meas}$ as a function of the nominal (P/Ti) yields the second relationship from a linear fit (Fig. 1):

$$(H/Ti)_{meas} = 4.2 + 1.6(P/Ti), \tag{2}$$

which, combined with Eq. (1), gives the following equation:

$$(O/Ti)_{calc} \approx 4.1 + 3.3(P/Ti). \tag{3}$$

From an extrapolation of the curve to P/Ti = 0, we obtain a chemical composition of TiO$_2$–2.1H$_2$O for the precipitate of hydrous titanium oxide. As written, the composition corresponds to the most condensed form of the hypothetical hydroxide Ti(OH)$_4$ resulting from the hydrolysis of the alkoxide Ti(OEt)$_4$. Also, this extrapolated value of 2.1 is higher than the experimental result (from thermogravimetric analysis) that yields TiO$_2$–1.05H$_2$O, but this value depends on the drying conditions (time, temperature, air moisture). Nevertheless, the actual precipitate obtained by hydrolysis of Ti(OEt)$_4$ with an excess of water should be an intermediate between the hydroxide and the hydrous oxide. We can conclude from Eqs. (2) and (3) that, when the amount of phosphate progressively increases, the following substitution occurs in the precipitate:

$$O^{2-} \longrightarrow HPO_4^{2-} + 0.3H_2O$$

$$\left(or\ 2OH^- \longrightarrow HPO_4^{2-} + 1.3H_2O\right).$$
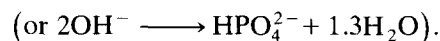
This composition change leads from the hydrous oxide to a composition Ti(HPO$_4$)$_2$–2.7H$_2$O for P/Ti = 2. This last composition is reminiscent of the αTi(HPO$_4$)$_2$–H$_2$O crystalline structure in which titanium has an octahedral coordination formed by six oxygens from six different HPO$_4$

[1]. Indeed, this layered crystalline phase forms upon aging the precipitate when $P/Ti \geqslant 2$.

Thus, we conclude that the chemical analysis shows a progressive substitution of oxide/hydroxide ligands (Ti–OH, Ti–O–Ti) by phosphate, up to the ratio $P/Ti = 2$ at which the most stable coordination of Ti (sixfold) is saturated by phosphate ligands (HPO_4^{2-}).

3.2. Titanium coordination

3.2.1. Analysis of the pre-edge

The X-ray absorption pre-edge (Fig. 2) corresponds to electronic transitions from the 1s (of A_{1g} symmetry) towards final states, which are essentially Ti 3d-bound states. If the nature of the A1 structure remains uncertain, the A_2 and A_3 structures may be assigned to dipolar forbidden, quadrupolar allowed $A_{1g} \rightarrow T_{2g}$ (A_2) and $A_{1g} \rightarrow E_g$ (A_3) transitions. The intensity of these absorptions is closely related to the symmetry of the titanium site. Dipolar forbidden when an inversion center is present, they become allowed when the local point group symmetry allows some mixing with p states (C_{4v} or Td symmetry for example).

Moreover, the presence of these three small peaks is unambiguously due to the absorption of a titanium in a sixfold coordination [16]. The dipolar and quadrupolar contributions to the absorption spectrum of TiO_2 (rutile) have been recently analyzed by Uozumi et al. [13]. The two peaks located at higher energy are assigned to the $1s \rightarrow t_{2g}$ (peak A2) and $1s \rightarrow e_g$ (peak A3) dipolar transitions. The two quadrupolar absorption peaks are A1 and a peak superimposed to A2 [13]. The decrease of the intensity of the peak A2 as a function of the P/Ti ratio (Fig. 3) indicates an increasing symmetry of the ligands around Ti as well as a smaller amount of mixing between Ti(3d) and O(2p) orbitals when Ti–O–Ti bonds are progressively replaced by Ti–O–P. At the $P/Ti = 2$ ratio (amorphous as well as crystalline), only the weak quadrupolar transitions are observed. This observation indicates a stereochemistry close to a symmetry with an inversion center. However, apart from a structure obtained from a Rietveld fit on a powder pattern [17], the results

of which may not be precise enough to be used in this discussion, the only information available on this structure is that it is isostructural with $\alpha Zr(HPO_4)_2$–H_2O. This last compound contains Zr having a slightly distorted octahedral coordination.

If we assume that the precipitates contain HPO_4^{2-} groups that can use three oxygens for binding, the pure octahedral coordination using phosphates is only achieved for the $P/Ti = 2$ ratio. This is in agreement with the X-ray absorption. For lower ratios, the larger intensity of the dipolar absorptions indicates that there is an asymmetrical distribution of ligands (oxide, hydroxide and phosphate) also observed in the hydrous titanium oxide. Indeed, the amorphous hydrous titanium oxide has an absorption intensity quite high as compared with TiO_2 rutile [18]. This amorphous material may exhibit a large distribution of long and short bridging bonds (Ti–O–Ti or Ti–OH–Ti) and shorter terminal bonds (TiOH).

In the case of the gels, the dipolar absorption has a quite high intensity even for the $P/Ti = 2$ ratio (Fig. 2(b)). In this case, the ligands around Ti must be distributed between alkoxy and phosphate groups. This indicates that the coordination is not as symmetrical as in the dried samples and does not consist purely of phosphates.

3.2.2. Analysis of the EXAFS

These results are consistent with the EXAFS analysis which indicates, in the case of the gels, a distribution of Ti–O bonds between two different lengths (Fig. 4). The short bonds (1.85 Å) are reminiscent of unsubstituted terminal Ti–OR groups [18], whereas the long bonds (2.06 Å) could be bridging Ti–O(P or Ti) bonds.

The value of 1.95 Å obtained for the layered crystalline phase ($\alpha Ti(HPO_4)_2$–H_2O) is characteristic of the Ti–O–P distance and is similar to that observed for the $P/Ti = 2$ precipitate (1.98 Å). Therefore, we conclude that phosphates have substituted all the alkoxy groups above this ratio. In good agreement with the analysis of the absorption edge, the decrease of the Ti–O distance from 2.03 to 1.96 Å, for the precipitates, can be attributed to a continuous evolution of the Ti

coordination from the (O, OH and H_2O) environment to a (HPO_4) coordination. However, we may observe a macroscopic mixture of amorphous hydrated TiO_2–nH_2O and amorphous titanium phosphate, the proportion of which changes with the P/Ti ratio. This hypothesis would not explain that all Ti are precipitated upon addition of phosphoric acid in a ratio much lower than 2 without hydrolysis. Moreover, it is ruled out by the ^{31}P solid state MAS-NMR and Raman spectroscopies results.

3.3. Raman spectroscopy

Indeed, the Raman spectrum observed at the ratio P/Ti = 1 is not a mixture of the spectra observed for P/Ti = 0 and P/Ti = 2 (Fig. 10). Moreover, a strong peak around 750 cm^{-1} appears for the intermediate compositions. This frequency is characteristic of many vibration modes such as P–O–P symmetric stretch [19,20]. However, on the chemical point of view, the condensation of pyrophosphate groups is very improbable without heating and their vibration intensity should be much weaker. Such vibration frequency has been also attributed by many authors to the Ti–O stretching mode of TiO_4 tetrahedral units as observed in melt-cooled Na_2O–TiO_2–P_2O_5 [20] or TiO_2–SiO_2 glasses [21]. The same vibration frequency is also observed in the Ba_2TiO_4 crystalline phase which contains tetrahedral TiO_4 units [22]. However, in our case, we believe that they are more appropriate to short, non-bridging Ti–O bonds, independent of the nature of the Ti coordination. First, from our EXAFS study, and from the current knowledge of the condensation of Ti alkoxides [23], higher coordination numbers have to be present in the precipitates. Moreover, a correlation between the shortest Ti–O bond and the vibration frequency has been given by Sakka et al. [22]. They concluded that "the wavenumber in the Raman spectra of titanate crystals reflect the shortest Ti–O distance or the distortion of polyhedra and they do not directly correspond to the coordination number of Ti^{4+} ions". From their work, the frequency of 750 cm^{-1} corresponds to Ti–O bond lengths around

1.85 Å, consistent with the short distances observed in EXAFS in the gels. These bonds should correspond to Ti–O_{nb} (non-bridging oxygen) [22]. Such a signal is also reported by Chernokurov et al. who studied $TiOHPO_4$–nH_2O crystallized from hydrothermal synthesis [24]. They also attribute this vibration to a short titanyl Ti = O or terminal Ti–OH. Therefore, the vibration observed at 750 cm^{-1} may be characteristic of short Ti–O bonds although the distance of 1.85 Å is rather long to be considered as a titanyl group (it is 1.75 Å for the shortest Ti–O bond of $KTiOPO_4$).

From this Raman study, we conclude that introduction of small amount of phosphates in amorphous precipitates of titanium oxy-phosphates introduces a large distortion of TiO_6 octahedra as compared with pure amorphous TiO_2–nH_2O obtained from hydrolysis condensation. Upon increasing the P/Ti ratio, coordination becomes more symmetrical.

3.4. Phosphorus coordination

The progressive change of the ^{31}P NMR signal composition with P/Ti ratio as well as the distribution among a large number of different peaks (Fig. 8) is an argument in favour of the homogeneous distribution of phosphates in the samples. Indeed, a mixture of two microphases would only give two sharp peaks, the relative intensity of which would depend on the P/Ti ratio.

By comparison with the chemical shifts of different nuclei such as Si in silicates [25], spectra can be analyzed by associating each ^{31}P signal with a different connectivity of the phosphates ions towards Ti. Similar discussions have also been developed in the literature with the NMR of aluminum silicates [26] or antimony phosphates [27]. However, the relative position of cations as well as the change of the O–P–O angles may have similar effects on the chemical shift [28]. Therefore, our correlation is valid if we assume that the PO_4 groups are almost identical (bond angles, P–O distances) except for the distance of Ti atoms to the bridging oxygens. Then, a first straightforward naive attribution of the

peaks that have been obtained from the fits would
be

≈ 0 ppm free or adsorbed H_3PO_4;

≈ -5 ppm H_3PO_4 or H_2PO_4 with 1P–O–Ti
bound;

≈ -9 ppm H_2PO_4 or HPO_4 with 2P–O–Ti
bounds;

-15 to -22 ppm HPO_4 or PO_4 with 3 P–O–Ti
bounds (several peaks observed between -14.7
and -21.7 ppm);

≈ -27 ppm PO_4 with 4 P–O–Ti bounds (easily
observed in the sample $P/Ti = 3/2$, Fig. 8). In
agreement with these attributions, the signal of
phosphates coordinated to four different titanium
atoms is observed at -27 ppm in $NaTi_2(PO_4)_3$,
whereas it is observed at -32.5 in $\gamma TiPO_4$
(H_2PO_4)–$2H_2O$ [17]. Similarly, the signal that we
attribute to phosphate linked to three titanium
atoms in the amorphous sample corresponding to
$P/Ti = 2$ is observed at -21.7 ppm, quite the
same position as in crystalline $\alpha Ti(HPO_4)_2$–H_2O
(-19.4 ppm). The small discrepancy between
these values may be ascribed to slightly different
hydrogen bonds related to the difference in crys-
tallinity more than to a different nature of the
phosphate coordination. Protonation of phos-
phate groups has only a slight effect on the chem-
ical shift of phosphate species, as generally ob-
served in the solutions (± 2 ppm). In our amor-
phous samples, a major peak is observed around
-9 ppm for the $P/Ti = 1$ ratio. This is reminis-
cent of the H_2PO_4 groups observed at -9 ppm
in $\gamma TiPO_4(H_2PO_4)$–$2H_2O$ [17] and at -8 ppm in
the $TiO(OH)(H_2PO_4)$ phase recently isolated by
Li and Wittingham [29].

In all cases, the stronger peaks are either -9
ppm around the $P/Ti = 1$ ratio or -21.7 ppm
which is observed quite pure for the $P/Ti = 2$
ratio. These signals may correspond to the most
stable microscopic configurations corresponding
to stable phases crystallized from the H_2O–
TiO_2–H_3PO_4 system, $\alpha Ti(HPO_4)_2$–H_2O [1] and
$TiO(OH)(H_2PO_4)$ [29].

We can derive the average connectivity of
phosphate towards Ti from our attributions of the
peaks and the percentages of each signal given in
Fig. 9(a). This connectivity, when multiplied by
the P/Ti ratio, yields the number of phosphate

anions coordinated to each Ti and the results are
reported in Fig. 9(b). With this analysis, we ob-
serve a too low coordination of phosphate to-
wards Ti, since we concluded from the X-ray
absorption study that the coordination of tita-
nium should be of six oxygens from the phos-
phates for $P/Ti = 2$ and that only 4.5 are ob-
served in Fig. 9(b). Moreover, from our attribu-
tions of peaks and from Fig. 9(a) we observe that
the lower the P/Ti ratio, the lower the average
number of Ti connected to each phosphate.
Therefore, this trend implies that our naive attri-
bution of peaks to different connectivities of the
phosphate ions corresponds only partially to real-
ity. However, phosphates considered in our anal-
ysis to be bound to only one or two Ti may act as
a chelate and bind through two oxygens to the
same Ti. Nevertheless, in these amorphous mate-
rials, it is sometimes difficult to separate the
phosphates into discrete classes of connectivity,
since the Ti–O–P distances and bond angles may
vary continuously.

Moreover, phosphates which are connected to
four Ti atoms in the $KTiOPO_4$ structure exhibit
NMR signals at 1.9 and 0.6 ppm in disagreement
with our conclusions above that would attribute
these peaks to free phosphates. Cheetham and
co-workers [30,31] have developed an interesting
approach for correlating the ^{31}P NMR chemical
shifts to the structural parameters of inorganic
phosphates. Their analysis is based on the use of
bond strengths derived from the studies of Brown
and Shannon [32]. It results from this analysis
that the chemical shift moves downfield as the
bond strengths at oxygen decreases. Therefore,
species observed at higher chemical shift may be
phosphates exhibiting longer bond distances to Ti
atoms rather than lower connectivities. For the
low P/Ti ratios, the Ti–O–P bonds may be asso-
ciated to part of the large Ti–O distances ob-
served at 2.05 Å by EXAFS. This also implies
that, in order to achieve the usual bond strength
at the Ti atoms ($+4$) [32], such long Ti–O(–P)
distances must be associated to shorter Ti–O
bonds around the same Ti.

Upon increasing the P/Ti ratio, the number
of short Ti–O bonds decreases (Fig. 5). They are
progressively replaced by longer P–O–Ti bonds.

The very high hyperpolarizability of the short Ti–O bonds offers possible applications in the domain of non-linear optical or electro-optical properties [3,4]. As shown here; precipitation from solutions allows the synthesis of homogeneous systems with high TiO_2 contents, whereas conventional synthesis from the melt offers a limited vitreous domain. However, due to the rough precipitation conditions that we have used in this work, our samples are not transparent. Controlling the polymerization of titanium phosphate through a better condensation and obtaining transparent samples is the subject of another part of our work that is described elsewhere [7].

4. Conclusions

Reaction of orthophosphoric acid with titanium alkoxides yields amorphous precipitates that consist of a polymeric network of titanium linked by phosphate and unsubstituted alkoxy groups. Upon hydrolysis and drying, the remaining alkoxy groups are replaced by Ti–OH groups and condensation of these groups into Ti–O–Ti bonds occurs.

From the progressive change in the ^{31}P NMR spectra and from the Ti EXAFS results, we conclude that the distribution of Ti and P in the amorphous precipitates is homogeneous at the molecular level and continuously varies for ratios $0.5 \leqslant P/Ti \leqslant 2$.

The analysis of the ^{31}P NMR signals shows a large distribution of phosphates among different sites. The nature of these sites remains to be analyzed more precisely.

For the lowest ratios, Ti has a distorted sixfold coordination with short terminal Ti–O(H) bonds associated to long Ti–O–P and Ti–O(H)–Ti locally similar to a hydroxy-orthophosphate of titanium $(TiO(OH)(H_2PO_4)-nH_2O)$. The presence of short Ti–O bonds is confirmed by Raman spectroscopy.

For $P/Ti = 2$, the most stable configuration is a pure octahedral coordination of Ti surrounded with six different HPO_4 groups. For this ratio, the amorphous precipitate has a local structure very similar to the crystalline layered compound $\alpha Ti(HPO_4)_2-H_2O$.

References

[1] G. Albert, P.C. Galli, U. Costantino and E. Toracca, J. Inorg. Chem. 29 (1967) 571.

[2] M.A. Subramanian, R. Subramanian and A. Clearfield, Solid State Ionics 18&19 (1986) 562.

[3] G.D. Stucky, M.L.P. Phillips and T.E. Gier, Chem. Mater. 1 (1989) 492.

[4] C. Duchesne, E. Fargin, R. Olazcuaga, G. LeFlem, S. Krimi, I. Mansouri and A. ElJazouli, J. Phys. (Paris) IV Colloq. C2 2 (1992) C2-261.

[5] B.E. Sringett, J. Non-Cryst. Solids 15 (1974) 179.

[6] J. Livage, P. Barboux, M.T. Vandenborre, C. Schmutz and F. Taulelle, J. Non-Cryst. Solids 147&148 (1992) 18.

[7] C. Schmutz, E. Basset, P. Barboux and J. Maquet, J. Mater. Chem. 3 (1993) 393.

[8] C. Schmutz, E. Basset and P. Barboux, J. Phys. (Paris) III 3 (1993) 757.

[9] A. Michalowicz, EXAFS pour le Mac, Logiciels pour la Chimie (Société Française de Chimie, Paris, 1991) p. 102.

[10] A.G. McKale, B.W. Veal, A.P. Paulikas, S.K. Khan and G.S. Knapp, J. Am. Chem. Soc. 110 (1988) 3763.

[11] A. Michalovicz, M. Verdaguer, Y. Mathey and R. Clément, in: Topics in Current Chemistry, Vol. 145 (Springer, Berlin, 1988) p. 109.

[12] J. Goulon, P. Friant, C. Goulon-Ginet, A. Coutsolelos and R. Guilard, Chem. Phys. 83 (1984) 367.

[13] T. Uozumi, K. Okada, A. Kotani, O. Durmeyer, J.P. Kappler, E. Beaurepaire and J.C. Parlebas, Europhys. Lett. 18 (1992) 85.

[14] T. Furukawa and W.B. White, Phys. Chem. Glasses 20 (1979) 69.

[15] S.E. Horsley, D.V. Nowell and D.T. Stewart, Spectrochim. Acta 30A (1974) 535.

[16] T. Dumas and J. Petiau, J. Non-Cryst. Solids 81 (1986) 201.

[17] A.N. Christensen, E.G. Krogh Andersen, I.G. Krogh Andersen, G. Alberti, M. Nielsen and S.M. Lehmann, Acta Chem. Scand. 44 (1990) 865.

[18] F. Babonneau, S. Doeuff, A. Léaustic, C. Sanchez, C. Cartier and M. Verdaguer, Inorg. Chem. 27 (1988) 3166.

[19] D.R. Tallant and C. Nelson, Phys. Chem. Glasses 27 (1986) 75.

[20] L.A. Farrow and E.M. Vogel, J. Non-Cryst. Solids 143 (1992) 59.

[21] M.F. Best and R.A. Condrate, J. Mater. Sci. Lett. 4 (1985) 994.

[22] S. Sakka, F. Miyaji and K. Fukumi, J. Non-Cryst. Solids 112 (1989) 64.

[23] S. Doeuff, M. Henry, C. Sanchez and J. Livage, J. Non-Cryst. Solids 89 (1987) 84.

[24] N.G. Chernokurov, I.A. Korshunov and M.I. Zhuk, Russ. J. Inorg. Chem. 27 (1982) 1728.

[25] A.R. Grimmer and V. Haubenreisser, Chem. Phys. Lett. 99 (1983) 487.

[26] E. Lippmaa, M. Magi, A. Samoson, M. Tarmak and G. Engelhardt, J. Am. Chem. Soc. 103 (1981) 4992.

[27] F. Taulelle, C. Sanchez, J. Livage, A. Lachgard and Y. Piffard, J. Phys. Chem. Solids 49 (1988) 299.

[28] P. Losso, B. Schnabel, C. Jäger, U. Sternberg, D. Stachel and D.O. Smith, J. Non-Cryst. Solids 143 (1992) 265

[29] Y.J. Li and S.J. Wittingham, Solid State Ionics 63–65 (1993) 391.

[30] S.J. Crennell, J.J. Owen, C.P. Grey, A.K. Cheetham, J.A. Kaduk and R.H. Jarman, J. Mater. Chem. 1 (1991) 113.

[31] A.K. Cheetham, N.J. Clayden, C.M. Dobson and R.J.B. Jakeman, J. Chem. Soc. Chem. Commun. (1986) 195.

[32] I.D. Brown and R.D. Shannon, Acta Crystallogr. A29 (1973) 226.